

BODY SIZE

Why whales are big but not bigger: Physiological drivers and ecological limits in the age of ocean giants

J. A. Goldbogen^{1*}, D. E. Cade¹, D. M. Wisniewska¹, J. Potvin², P. S. Segre¹, M. S. Savoca¹, E. L. Hazen^{1,3,4}, M. F. Czapanskiy¹, S. R. Kahane-Rapport¹, S. L. DeRuiter⁵, S. Gero⁶, P. Tønnesen⁶, W. T. Gough¹, M. B. Hanson⁷, M. M. Holt⁷, F. H. Jensen⁸, M. Simon⁹, A. K. Stimpert¹⁰, P. Arranz¹¹, D. W. Johnston¹², D. P. Nowacek¹³, S. E. Parks¹⁴, F. Visser^{15,16,17}, A. S. Friedlaender⁴, P. L. Tyack¹⁸, P. T. Madsen^{6,19}, N. D. Pyenson^{20,21}

The largest animals are marine filter feeders, but the underlying mechanism of their large size remains unexplained. We measured feeding performance and prey quality to demonstrate how whale gigantism is driven by the interplay of prey abundance and harvesting mechanisms that increase prey capture rates and energy intake. The foraging efficiency of toothed whales that feed on single prey is constrained by the abundance of large prey, whereas filter-feeding baleen whales seasonally exploit vast swarms of small prey at high efficiencies. Given temporally and spatially aggregated prey, filter feeding provides an evolutionary pathway to extremes in body size that are not available to lineages that must feed on one prey at a time. Maximum size in filter feeders is likely constrained by prey availability across space and time.

Large body size can improve metabolic and locomotor efficiency. In the oceans, extremely large body size evolved multiple times, especially among edentulous filter feeders that exploit dense patches of small-bodied prey (1, 2). All of these filter feeders had smaller, toothed ancestors that targeted much larger, single prey (3, 4). The ocean has hosted the rise and fall of giant tetrapods since the Triassic, but the largest known animals persist in today's oceans, comprising multiple cetacean lineages (5–8). The evolution of specialized foraging mechanisms that distinguish the two major whale clades—biosonar-guided foraging on individual prey in toothed whales (Odontoceti) and engulfment filter feeding on prey aggregations in baleen whales (Mysticeti)—likely led to the diversification of crown cetaceans during the Oligocene (~33 to 23 million years ago). The origin of these foraging mechanisms preceded the recent evolution of the largest body sizes (9, 10), and the diversification of these mechanisms across this body size spectrum was likely enhanced by scale-dependent predator-prey processes (11). It is hypothesized that toothed whales evolved larger body sizes to enhance diving capacity and exploit deep-

sea prey using more powerful biosonar (12), whereas baleen whales evolved larger sizes for more efficient exploitation of abundant, but patchily distributed, small-bodied prey (13). Cetacean foraging performance is constrained by diving physiology because cetaceans must balance two spatially decoupled resources: oxygen at the sea surface and higher-quality food at depth (14). In both lineages, large body size confers an ecological benefit that arises from the scaling of fundamental physiological processes; in some species, anatomical, molecular, and biochemical adaptations further enhance diving capacity (13). As animal size increases, mass-specific oxygen storage is constant yet mass-specific oxygen usage decreases (13). Therefore, larger air-breathers should have greater diving capacity and thus be capable of feeding for longer periods at a given depth, leading to higher feeding rates overall. In theory, this leads to relatively greater dive-specific energy intake with increasing body size; and, with unlimited prey at the scale of foraging grounds and seasons, larger divers will also exhibit greater energetic efficiencies (i.e., energy intake relative to energy use) while foraging. We hypothesized that the energetic efficiency of foraging will increase with body

size because larger animals will have greater diving capacities and more opportunities to feed more frequently per dive. Filter-feeding baleen whales will exhibit relatively higher efficiencies compared with single-prey-feeding toothed whales, because they can exploit greater biomass at lower trophic levels. This study uses whale-borne tag data to provide a comparative test of these fundamental predictions.

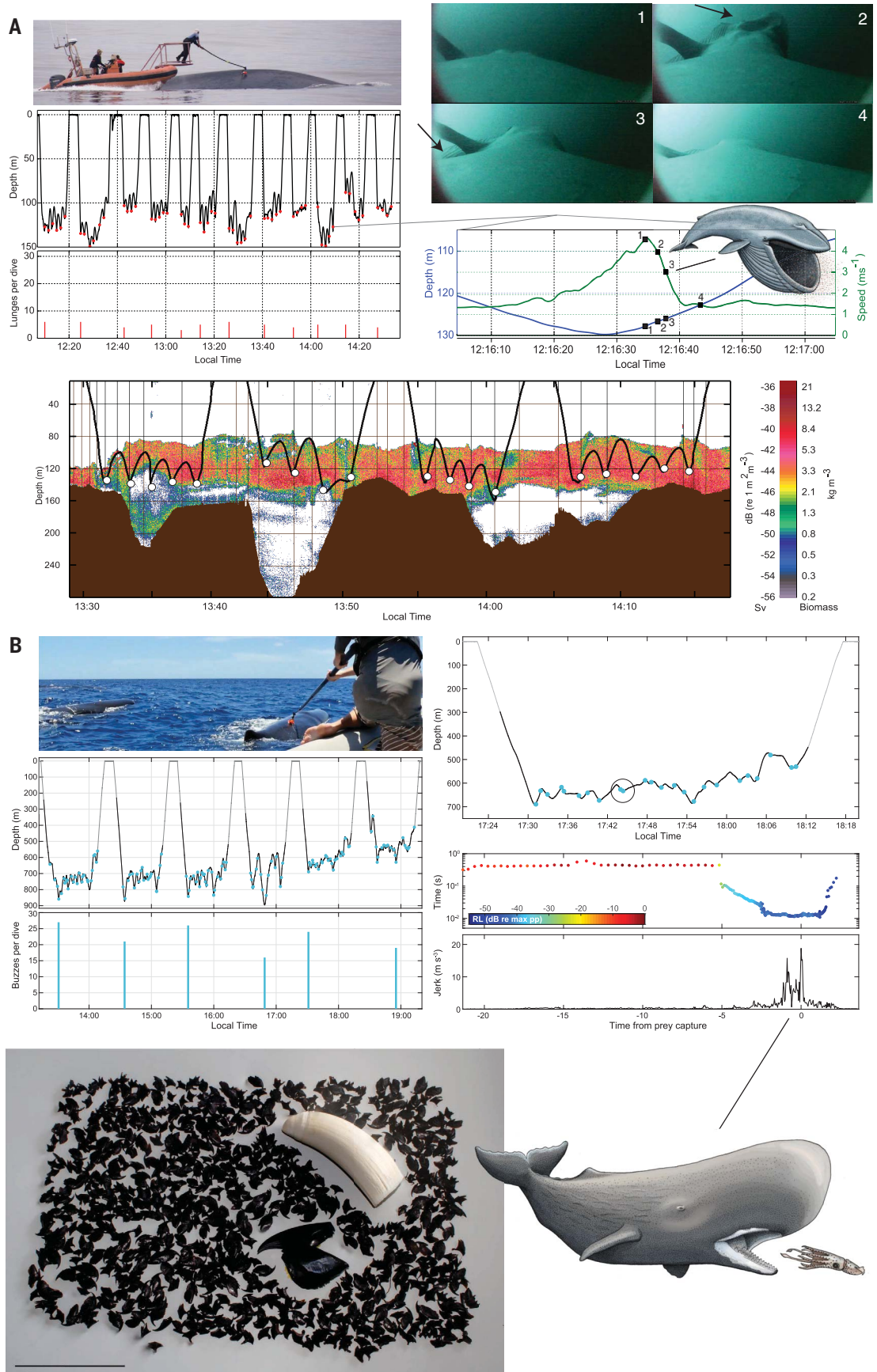
Our direct measures of foraging performance using multisensor tags (Fig. 1) show that the largest odontocetes, such as sperm whales (*Physeter macrocephalus*) and beaked whales (Ziphiidae), exhibited high feeding rates during long, deep dives (Fig. 2). By investing time and energy in prolonged dives, these whales accessed deeper habitats that contained less mobile and potentially more abundant prey (15), such as weakly muscularized, ammoniacal squid. Conversely, rorqual whales performed fewer feeding events per dive despite their large body size, because they invested large amounts of energy to engulf larger volumes of prey-laden water (16). The energetic efficiency (E_E , defined as the energy from captured prey divided by the expended energy, including diving costs and postdive recovery) is determined largely by the number of feeding events per dive (Fig. 2) and the amount of energy obtained during each feeding event (Fig. 3). This amount of energy obtained per feeding event was calculated from prey type and size distributions historically found in the stomachs of odontocetes (except for killer whales, for which we used identified prey remains from visually confirmed prey capture events), as well as the acoustically measured biomass, density, and distribution of krill at rorqual foraging hotspots (17). Our results show that although larger odontocetes appear to feed on larger prey relative to the prey of smaller, toothed whales, these prey were not disproportionately larger (Fig. 3 and table S11), and toothed whales did feed more frequently on this smaller prey type. Thus, the energy obtained from prey in a dive did not outweigh the increased costs associated with larger body size and deeper dives (fig. S2), thereby causing a decrease in E_E with increasing body size in odontocetes (Fig. 4). In contrast, the measured distribution and density of krill biomass suggests that larger rorquals are not prey-limited at the scale of individual dives. Because larger

¹Hopkins Marine Station, Department of Biology, Stanford University, Pacific Grove, CA, USA. ²Department of Physics, Saint Louis University, St. Louis, MO, USA. ³Environmental Research Division, National Oceanic and Atmospheric Administration, Southwest Fisheries Science Center, Monterey, CA, USA. ⁴Institute of Marine Sciences, University of California, Santa Cruz, Santa Cruz, CA, USA. ⁵Mathematics and Statistics Department, Calvin University, Grand Rapids, MI, USA. ⁶Zoophysiology, Department of Bioscience, Aarhus University, Aarhus, Denmark. ⁷Conservation Biology Division, Northwest Fisheries Science Center, National Marine Fisheries Service, National Oceanic and Atmospheric Administration, Seattle, WA, USA. ⁸Biology Department, Woods Hole Oceanographic Institution, Woods Hole, MA, USA. ⁹Greenland Climate Research Centre, Greenland Institute of Natural Resources, Nuuk, Greenland. ¹⁰Moss Landing Marine Laboratories, Moss Landing, CA, USA. ¹¹Biodiversity, Marine Ecology and Conservation Group, Department of Animal Biology, University of La Laguna, La Laguna, Spain. ¹²Nicholas School of the Environment, Duke University Marine Laboratory, Beaufort, NC, USA. ¹³Pratt School of Engineering, Duke University, Durham, NC, USA. ¹⁴Department of Biology, Syracuse University, Syracuse, NY, USA. ¹⁵Department of Freshwater and Marine Ecology, IBED, University of Amsterdam, Amsterdam, Netherlands. ¹⁶Department of Coastal Systems, NIOZ and Utrecht University, Utrecht, Netherlands. ¹⁷Kelp Marine Research, Hoorn, Netherlands. ¹⁸Sea Mammal Research Unit, School of Biology, Scottish Oceans Institute, University of St Andrews, St Andrews, UK. ¹⁹Aarhus Institute of Advanced Studies, Aarhus University, DK-8000 Aarhus C, Denmark. ²⁰Department of Paleobiology, National Museum of Natural History, Washington, DC, USA. ²¹Department of Paleontology and Geology, Burke Museum of Natural History and Culture, Seattle, WA, USA.

*Corresponding author. Email: jergold@stanford.edu

Fig. 1. Whale tag data quantifies foraging performance.

(A) Blue whale suction-cup tagging using a rigid-hulled inflatable boat and a carbon fiber pole (upper left). Tag data from a blue whale showing 12 consecutive foraging dives and the number of lunge-feeding events per dive (left). Inset (right) shows the kinematic signatures used to detect lunge-feeding events (with an increase in speed and upward movement before lunging) and simultaneous video frames that directly confirm engulfment [images 1 to 4: 1, prior to mouth opening; 2, maximum gape (shown by arrow); 3, maximum extension of the ventral groove blubber (shown by arrow); and 4, after mouth closure during the filter phase]. (Bottom) Example of time-synchronized dive profile and the estimated biomass as a function of depth (17), grid lines are 147 m by 40 m. Prey mapping data were used to estimate the distribution of krill densities targeted by tagged whales. **(B)** Sperm whale suction-cup tagging (upper left) and six foraging dives with feeding events (thicker lines denote echolocation activity). Middle right panels show the acoustic interclick interval (ICI) and kinematic signatures (jerk, or rate of acceleration) used to infer feeding events at depth. The photograph on the bottom left shows examples of cephalopod beaks (single large beak, *Mesonychoteuthis hamiltoni*; many small beaks, *Gonatus fabricii*) found in the stomachs of sperm whales (lower left) that were used to estimate the size distributions of captured prey (sperm whale tooth and 10 cm line are also shown for scale, photo by Per Henriksen). Illustrations by Alex Boersma.



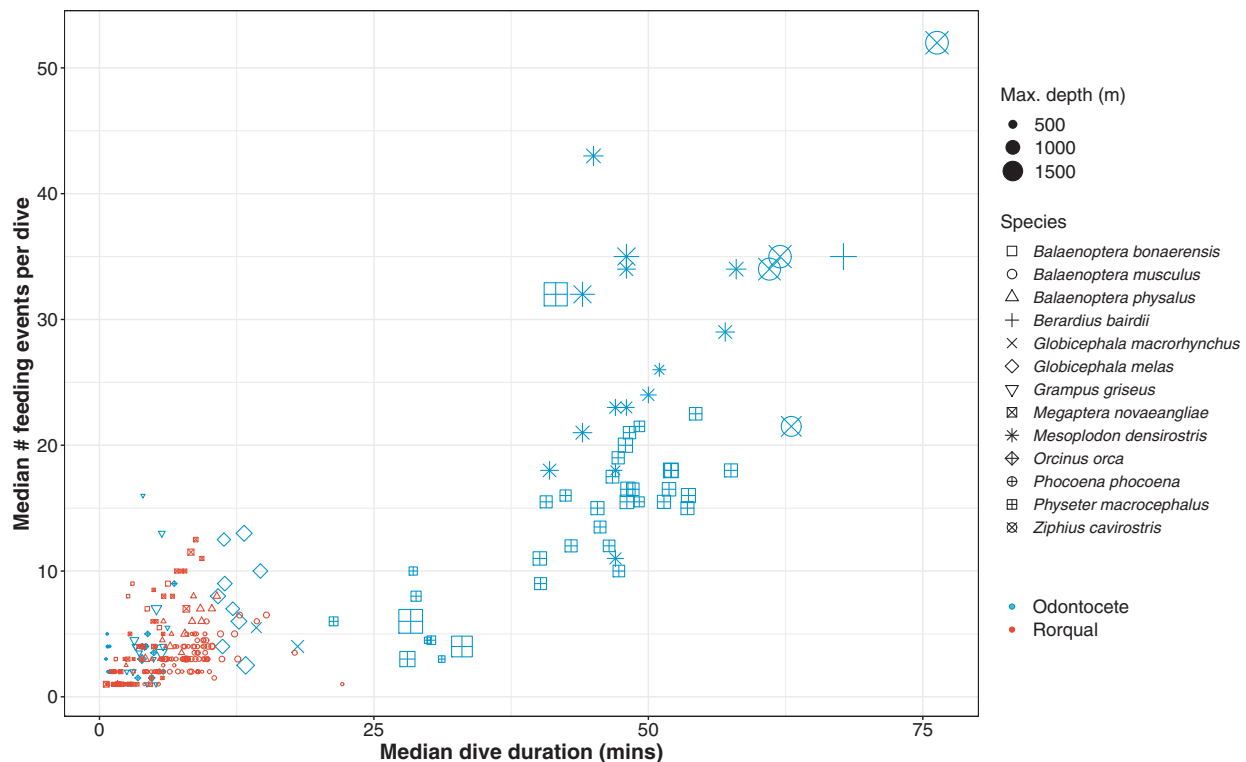


Fig. 2. Number of feeding events per foraging dive. Beaked whales (Ziphiidae) and some sperm whales (*P. macrocephalus*) exhibit high feeding rates during long, deep dives, whereas rorquals and delphinids feed less frequently during shorter, shallower dives. Balaenids were excluded from this analysis because they are continuous-ram filter feeders and do not exhibit discrete feeding events like rorquals and odontocetes.

rorquals have relatively larger engulfment capacities (16), rorquals exhibited much more rapid increases in energy captured from prey with increasing body size (Fig. 3). If they can detect and exploit the densest parts of an individual krill patch, as evidenced by their ability to maneuver more and increase feeding rates per dive when krill density is higher (14), then E_E should increase with body size (Fig. 4). These results were robust to assumptions about trait similarity from shared ancestry as well as the scaling of metabolic rate (MR), which we simulated over a wide range as $(MR \propto Mc^{0.45-0.75})$, where Mc is cetacean body mass.

The divergence in energetic scaling between rorquals and odontocetes that results from available prey has major implications for understanding the ecology and evolution of gigantism in marine ecosystems. For toothed whales, increasing body size leads to hyperallometric investment in biosonar structures that increase prey detection range (12). The largest living toothed whales today, sperm whales and beaked whales, independently evolved large body size to push their physiological limits for dive duration to spend more time feeding in the deep sea. The mesopelagic and bathypelagic realms are not only among the largest ecosystems on the planet, they also provide less competitive niches with fewer endothermic predators, providing opportunities

to capture high-value prey (18). Although sperm whales foraging on giant squids (Architeuthidae) persists as an iconic motif, giant squid beaks are rare in sperm whale stomachs at a global scale (19). However, sperm whale biosonar, owing to a hypertrophied nasal complex, is more powerful than beaked whale biosonar by approximately two orders of magnitude (12). This allows sperm whales to scan larger volumes of water and, in some regions, to find and chase very large prey. Sperm whales have higher attack speeds and reduced feeding rates per dive when foraging on giant squid (20), which contrasts with how sperm whales feed with slower speeds and higher feeding rates on smaller squid in other regions (21). This discrepancy suggests that larger prey will incur greater foraging costs, which partially offset the increased energetic gain. Smaller prey are usually more abundant than larger prey (22), so efforts to optimize foraging efficiency require the ability to detect the distribution of prey size, which favors the evolution of powerful sonar. Both beaked whales and many sperm whales in our study may have adopted a less risky strategy by targeting more reliable patches of cephalopods often at depths greater than 1000 m, thereby yielding up to 50 feeding events per dive (Fig. 2). Nevertheless, the ability of sperm whales to forage on the largest squid, when available, highlights an advan-

tage of their large size compared with beaked whales, which feed on smaller prey. Regardless of whether odontocetes target a few large prey or many small prey in individual dives, the energy gained from these deep-sea resources is ultimately constrained by the total amount of prey biomass that can be captured during a breath-hold dive. Therefore, prey availability is a key ecological factor that constrains body size and population density in these lineages.

By contrast, gigantism in mysticetes is advantageous because they exhibit positive allometry in filter-feeding adaptations that enable bulk consumption of dense prey patches (16). For the largest rorquals, each lunge captured a patch of krill with an integrated biomass and energetic content that exceeded, on average, those of the largest toothed whale prey by at least one order of magnitude (Fig. 3). This ability to process large volumes of prey-laden water, calculated as 100 to 160% of the whale's own body volume in the largest rorquals, underlies the high energetic efficiency of foraging, even when accounting for differences in body size (fig. S1). During lunge feeding, water and prey are engulfed in a matter of seconds and at speeds several times those of steady swimming (16). However, whales in a separate mysticete clade (Balaenidae), represented by bowhead whales (*Balaena mysticetus*) and right whales (*Eubalaena* spp.), do not feed in discrete events

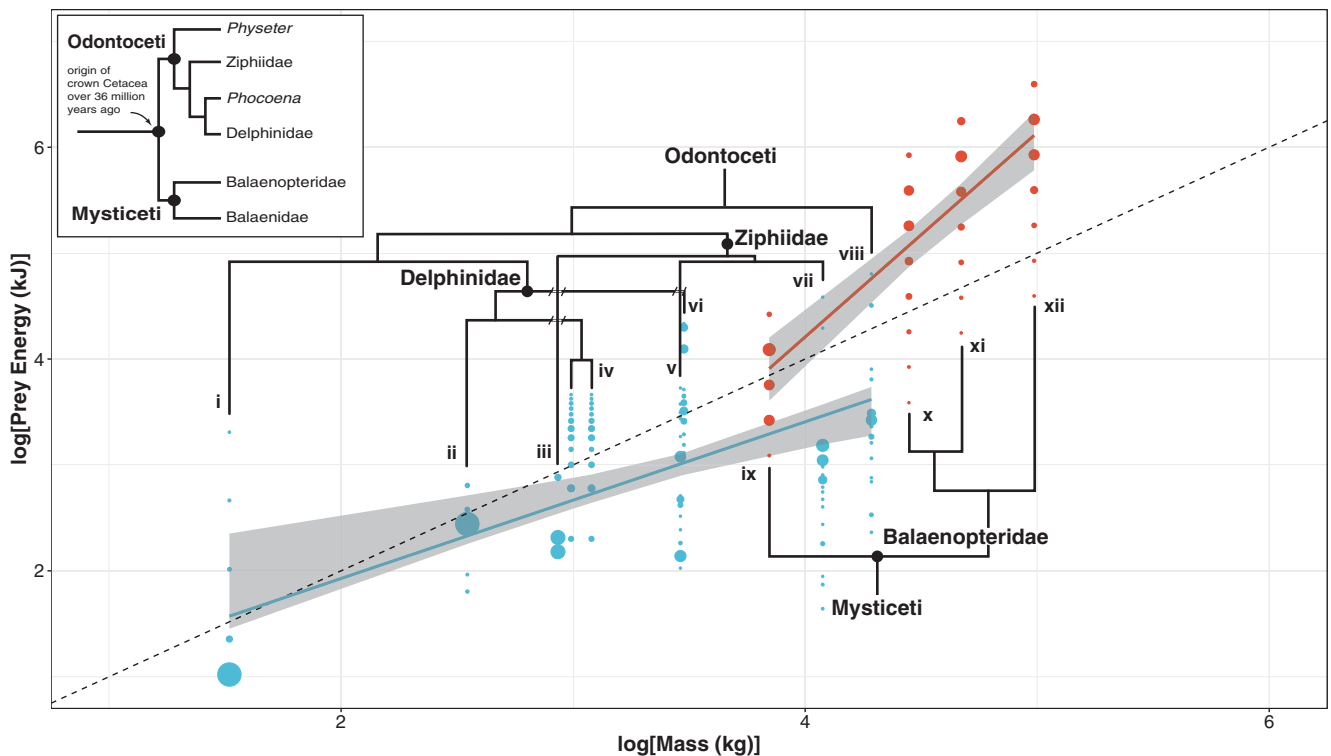


Fig. 3. Scaling of prey energy captured by toothed whales and rorqual whales during each feeding event. Estimates for prey energy (prey mass multiplied by prey energy density) obtained from each feeding event. For rorquals, the values indicate the integrated energy of all krill captured for each engulfment event. Symbol size indicates the relative frequency of occurrence based on stomach content data and prey mapping data for odontocetes and mysticetes, respectively. Symbol color is as in Fig. 2. The vertical spread of the data reflects the distribution of prey data for each species. This data was used to weight the regression fitted to species-specific means. The dashed line denotes isometry, indicating that larger toothed whales capture disproportionately less energy from prey ($y = 2.81x^{0.74}$, where y represents energy intake and x represents cetacean body mass), whereas larger rorquals capture disproportionately

larger prey energy, with increasing body size ($y = 0.000309x^{1.93}$). Generalized least squares regressions are shown with 95% confidence intervals (CI) (gray bands; see also table S11). The phylogenetic tree inset (with arbitrary branch lengths) shows evolutionary relationships (32) among species [(i) harbor porpoise, *Phocoena phocoena*; (ii) Risso's dolphin, *Grampus griseus*; (iii) Blainville's beaked whale, *Mesoplodon densirostris*; (iv) pilot whales, *Globicephala* spp.; (v) Cuvier's beaked whale, *Ziphius cavirostris*; (vi) killer whale, *Orcinus orca*; (vii) Baird's beaked whale, *Berardius bairdii*; (viii) sperm whale, *P. macrocephalus*; (ix) Antarctic minke whale, *Balaenoptera bonaerensis*; (x) humpback whale, *Megaptera novaeangliae*; (xi) fin whale, *Balaenoptera physalus*; (xii) blue whale, *Balaenoptera musculus*]. Balaenids were excluded from this analysis because they are continuous-ram filter feeders and do not exhibit discrete feeding events like rorquals and odontocetes.

but rather continuously ram prey-laden water through their baleen for up to several minutes at a time (23). The speed-dependent drag associated with continuous-ram filtration necessitates slow swimming speeds to minimize energy expenditure (23). This strategy may be optimized for foraging on smaller copepods that form less dense patches, thereby resulting in lower energetic efficiencies relative to similarly sized rorquals (Fig. 4). The high-speed dynamics of rorqual lunge feeding also generate high drag (16), but the rapid engulfment of dense krill patches yields higher efficiencies. Both continuous-ram filter-feeding and lunge-feeding mysticetes appeared to have independently evolved gigantism (>12 m body length) during an era of intensified wind-driven upwelling and glacial cycles, processes that characterize productive whale foraging hotspots in the modern oceans (9). Coastal upwelling intensity increases the number and density of aggregations of the relatively small-bodied

forage species (24) that make filter feeding energetically efficient (14). Our analyses point to filter feeding as a mechanism that explains the evolutionary pathway to gigantism because it enabled the high-efficiency exploitation of large, dense patches of prey.

The largest comparable vertebrates, sauropod dinosaurs, reached their maximum size on land about midway through their 140-million-year history, and their evolutionary patterns show no real limits to extreme size (25). If sauropod size was not limited by physical factors, such as gravity, hemodynamics, and bone mechanics (26), then it may have been ultimately constrained by energetics and food availability (27) rather than by an ability to access available food. In the marine environment, the combination of filter feeding and greater abundance of food likely facilitated the evolution of not only gigantic filter-feeding whales, but also that of several independent lineages of large filter-feeding elasmobranchs

(3, 6). Both filter-feeding sharks and mesothermic single-prey-feeding sharks exhibit greater body size compared with single-prey-feeding ectothermic sharks (3), suggesting parallel evolutionary trajectories with cetaceans in terms of gigantism and morphological adaptations that increase foraging capacity and net energy intake (4). The largest filter-feeding sharks are larger than mesothermic raptorial-feeding sharks, which may reflect either a lack of large prey as a limiting factor in today's oceans or an additional temperature-dependent metabolic constraint. Similarly, the larger size of baleen whales compared with filter-feeding sharks suggests an overall advantage for animals that exhibit both endothermy and filter-feeding adaptations, particularly in cold, productive habitats. The combination of high metabolic rates and the ability to short-circuit the food web with filter-feeding adaptations of low trophic levels (28), thereby facilitating

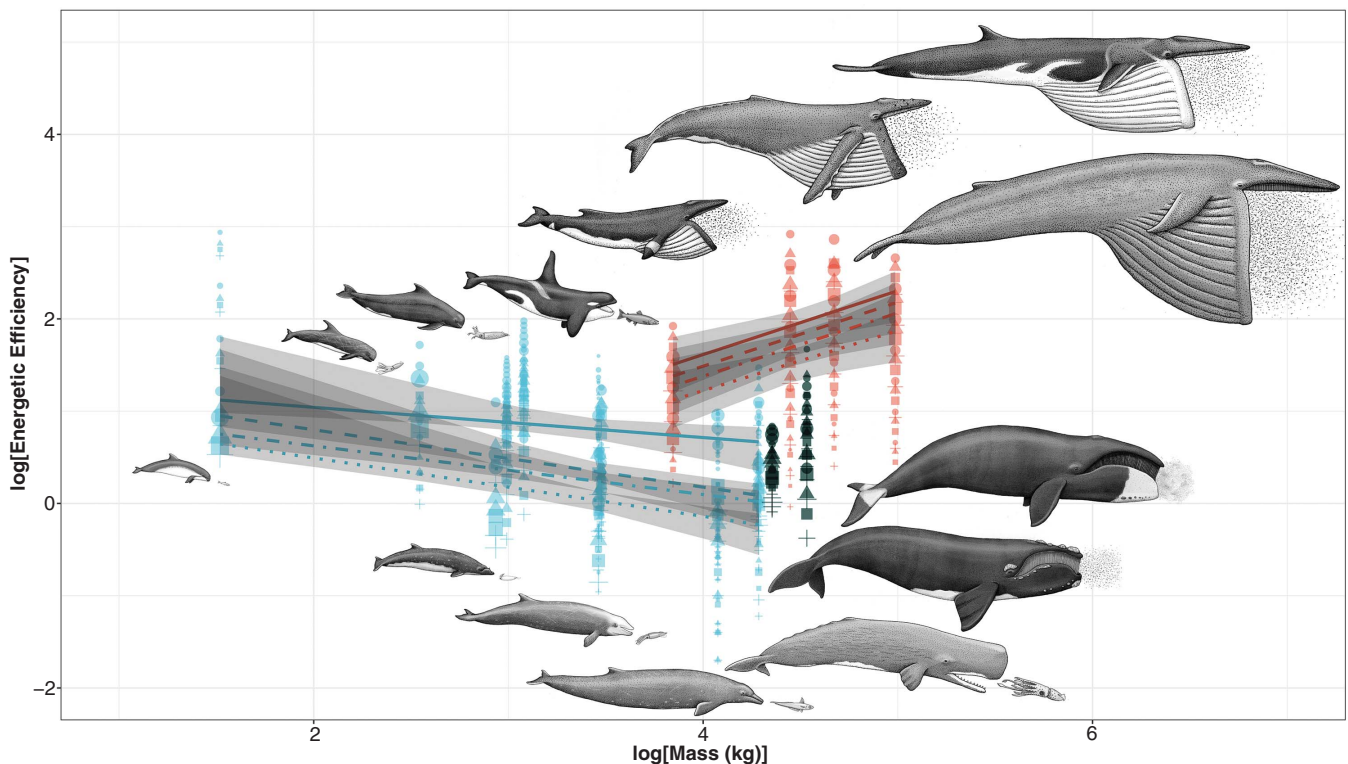


Fig. 4. Scaling of energetic efficiency for foraging dives and corresponding surface intervals. The energetic efficiency (E_E , defined as the energy from captured prey divided by the expended energy, including diving costs and postdive recovery) of foraging decreases in toothed whales (blue) but increases in rorqual whales lunge filter feeding on krill (red). Bowhead whales and right whales, which continuous-ram filter feed on copepods (green), exhibit lower energetic efficiencies compared with rorqual whales of similar size. These scaling relationships (table S11) are robust to assumptions about metabolic rate (plus symbols and dotted line,

$MR \propto Mc^{0.75}$; squares and dot-dash line, $MR \propto Mc^{0.68}$; triangles and dashed line, $MR \propto Mc^{0.61}$; circles and solid line, $MR \propto Mc^{0.45}$) that modulate the rate of energy expenditure of foraging. Regressions are shown with 95% CI (gray bands). The vertical spread of the data corresponds to prey quality distribution data (as in Fig. 3), with larger icons denoting greater proportions of observed values. The vertical spread of the data also reflects the distribution of prey data for each species. Log energetic efficiencies less than zero suggest that whales will be unable to survive on that prey type and quality alone. Illustrations by Alex Boersma.

the evolution of large body size in multiple lineages.

We have shown that cetacean gigantism is driven by the hyperallometry of structures that increase prey capture rates and energy intake in clades with divergent feeding mechanisms, despite the potential constraints to size. However, to maintain a high energetic efficiency at larger sizes, cetaceans must exploit either large individual prey or dense patches of small prey. Although the lack of large prey and the increasing costs of capturing such prey limits energetic efficiency of the largest toothed whales, our analyses suggest that large rorquals are not limited by the size and density of krill patches at the productive apex of their foraging seasons. How long these dense krill patches are available during the summer feeding season at higher latitudes, or throughout the rest of the year (29), may ultimately determine the amount of lipid reserves that can be used to fuel ocean basin-scale migrations as well as reproductive output at lower latitudes (30, 31). The size of the largest animals does not seem to be limited by physiology (5), but rather is limited by prey avail-

ability and the rate at which that prey can be exploited using the foraging mechanisms these whales have evolved.

REFERENCES AND NOTES

1. G. J. Vermeij, *PLOS ONE* **11**, e0146092 (2016).
2. C. R. McClain *et al.*, *PeerJ* **3**, e715 (2015).
3. C. Pimiento, J. L. Cantalapiedra, K. Shimada, D. J. Field, J. B. Smaers, *Evolution* **73**, 588–599 (2019).
4. M. Friedman, *Proc. R. Soc. B* **279**, 944–951 (2012).
5. W. Gearty, C. R. McClain, J. L. Payne, *Proc. Natl. Acad. Sci. U.S.A.* **115**, 4194–4199 (2018).
6. M. Friedman *et al.*, *Science* **327**, 990–993 (2010).
7. N. P. Kelley, N. D. Pyenson, *Science* **348**, aaa3716 (2015).
8. R. E. Fordyce, F. G. Marx, *Curr. Biol.* **28**, 1670–1676.e2 (2018).
9. G. J. Slater, J. A. Goldbogen, N. D. Pyenson, *Proc. R. Soc. B* **284**, 20170546 (2017).
10. O. Lambert *et al.*, *Nature* **466**, 105–108 (2010).
11. P. Domenici, *Comp. Biochem. Physiol. A* **131**, 169–182 (2001).
12. F. H. Jensen, M. Johnson, M. Ladegaard, D. M. Wisniewska, P. T. Madsen, *Curr. Biol.* **28**, 3878–3885.e3 (2018).
13. J. A. Goldbogen, P. T. Madsen, *J. Exp. Biol.* **221**, jeb166033 (2018).
14. E. L. Hazen, A. S. Friedlaender, J. A. Goldbogen, *Sci. Adv.* **1**, e1500469 (2015).
15. K. J. Benoit-Bird, B. L. Southall, M. A. Moline, *Proc. R. Soc. B* **283**, 20152457 (2016).
16. J. A. Goldbogen *et al.*, *Funct. Ecol.* **26**, 216–226 (2012).
17. See supplementary materials.
18. M. Clarke, C. Lu, *J. Mar. Biol. Assoc. U.K.* **55**, 165–182 (1975).
19. M. R. Clarke, *Philos. Trans. R. Soc. Lond. Ser. B* **351**, 1053–1065 (1996).
20. K. Aoki *et al.*, *Mar. Ecol. Prog. Ser.* **444**, 289–301 (2012).

21. A. Fais, M. Johnson, M. Wilson, N. Aguilar Soto, P. T. Madsen, *Sci. Rep.* **6**, 28562 (2016).
22. E. P. White, S. K. M. Ernest, A. J. Kerckhoff, B. J. Enquist, *Trends Ecol. Evol.* **22**, 323–330 (2007).
23. J. Potvin, A. J. Werth, *PLOS ONE* **12**, e0175220 (2017).
24. K. J. Benoit-Bird, C. M. Waluk, J. P. Ryan, *Geophys. Res. Lett.* **46**, 1537–1546 (2019).
25. R. B. Benson, G. Hunt, M. T. Carrano, N. Campione, *Palaeontology* **61**, 13–48 (2018).
26. P. M. Sander *et al.*, *Biol. Rev. Camb. Philos. Soc.* **86**, 117–155 (2011).
27. G. P. Burness, J. Diamond, T. Flannery, *Proc. Natl. Acad. Sci. U.S.A.* **98**, 14518–14523 (2001).
28. M. A. Tucker, T. L. Rogers, *Proc. R. Soc. B* **281**, 20142103 (2014).
29. C. K. Geijer, G. Notarbartolo di Sciarra, S. Panigada, *Mammal Rev.* **46**, 284–296 (2016).
30. E. Pirota *et al.*, *Am. Nat.* **191**, E40–E56 (2018).
31. R. Williams *et al.*, *ICES J. Mar. Sci.* **70**, 1273–1280 (2013).
32. J. H. Geisler, M. R. McGowen, G. Yang, J. Gatesy, *BMC Evol. Biol.* **11**, 112 (2011).

ACKNOWLEDGMENTS

We thank C. Taylor for Echoview processing and active acoustic data collection, A. Boersma for providing illustrations of cetacean species and their prey, and P. Henriksen for the photograph of squid beaks and the sperm whale tooth. We also thank W. Gearty for assistance with comparative phylogenetic analyses. **Funding:** This research was funded in part by grants from the National Science Foundation (IOS-1656676 and IOS-1656656; OPP-1644209 and 07-39483); the Office of Naval Research (N000141612477); and a Terman Fellowship from Stanford University. All procedures in the United States were conducted under approval of the National Marine Fisheries Service (permits

781-1824, 16163, 14809, 16111, 19116, 15271, and 20430); Canada DFO SARA/MML 2010-01/SARA-106B; National Marine Sanctuaries (MULTI-2017-007); Antarctic Conservation Act (2009-014 and 2015-011); and institutional IACUC committee protocols. Fieldwork, data collection, and data processing for *M. densirostris* were funded by the Office of Naval Research grants N00014-07-10988, N00014-07-11023, N00014-08-10990, N00014-18-1-2062, and 00014-15-1-2553, and the U.S. Strategic Environmental Research and Development Program Grant SI-1539. P.L.T. gratefully acknowledges funding from the MASTS pooling initiative (The Marine Alliance for Science and Technology for Scotland). MASTS is funded by the Scottish Funding Council (HR09011) and contributing institutions. Fieldwork, data collection, and data processing for *Globicephala melas* and data collection at the Azores were funded by the Office of Naval Research (ONR grants N00014-12-1-0410, N000141210417, N00014-15-1-2341, and N00014-17-1-2715); the Danish Council for Independent Research (award number 0602-02271B); the Dutch Research Council (award number 016.Veni.181.086); and a Semper Ardens Grant from the Carlsberg Foundation. For SRKW field work, we thank the NOAA Ocean Acoustics Program for providing funding and

C. Emmons, D. Giles, and J. Hogan for assistance in the field. For *P. macrocephalus*, fieldwork off Dominica was supported through a FNU fellowship from the Danish Council for Independent Research, supplemented by a Sapere Aude Research Talent Award, a Carlsberg Foundation expedition grant, a grant from Focused on Nature, and a CRE Grant from the National Geographic Society to S.G.; a FNU large frame grant; as well as a Villum Foundation Grant (to P.T.M.) with supplementary grants from Dansk Akustisk Selskab (to P.T.), Oticon Foundation (to P.T.), and Dansk Tennis Foundation (to P.T.). The Greenland data collection and analysis were funded by grants from the Oticon Foundation and the Carlsberg Foundation to M.S. Tagging work on *P. phocaena* was funded in part by the German Federal Agency for Nature Conservation (BfN) under contract Z1.2-530/2010/14 and the BfN-Cluster 7 "Effects of underwater noise on marine vertebrates." **Author contributions:** Overall idea, concept, and approach developed by J.A.G. Bioenergetic models developed by J.P. and implemented by J.A.G. Integration of data analysis and interpretation directed by J.A.G. Data analysis conducted and implemented by J.A.G., D.E.C., D.M.W., J.P., and P.S.S., with

statistical contributions by D.M.W., S.L.D., M.S.S., and E.L.H.. Manuscript written by J.A.G. and N.D.P. with contributions by D.E.C., D.M.W., J.P., P.L.T., P.T.M., and F.H.J. All authors read, edited, and discussed the manuscript and participated in data collection. **Competing interests:** The authors declare no competing interests. **Data and materials availability:** The data analyzed in this study will be available at the Stanford Data Repository ([sdr.stanford.edu](https://purl.stanford.edu/zk778rt5347)) immediately upon publication at <https://purl.stanford.edu/zk778rt5347>.

SUPPLEMENTARY MATERIALS

science.sciencemag.org/content/366/6471/1367/suppl/DC1
Materials and Methods
Figs. S1 and S2
Tables S1 to S11
References (33–185)

[View/request a protocol for this paper from Bio-protocol.](#)

3 May 2019; accepted 31 October 2019
10.1126/science.aax9044



Why whales are big but not bigger: Physiological drivers and ecological limits in the age of ocean giants

J. A. Goldbogen, D. E. Cade, D. M. Wisniewska, J. Potvin, P. S. Segre, M. S. Savoca, E. L. Hazen, M. F. Czapanskiy, S. R. Kahane-Rapport, S. L. DeRuiter, S. Gero, P. Tnnesen, W. T. Gough, M. B. Hanson, M. M. Holt, F. H. Jensen, M. Simon, A. K. Stimpert, P. Arranz, D. W. Johnston, D. P. Nowacek, S. E. Parks, F. Visser, A. S. Friedlaender, P. L. Tyack, P. T. Madsen, and N. D. Pyenson

Science, **366** (6471), .

DOI: 10.1126/science.aax9044

It's the prey that matters

Although many people think of dinosaurs as being the largest creatures to have lived on Earth, the true largest known animal is still here today—the blue whale. How whales were able to become so large has long been of interest. Goldbogen *et al.* used field-collected data on feeding and diving events across different types of whales to calculate rates of energy gain (see the Perspective by Williams). They found that increased body size facilitates increased prey capture. Furthermore, body-size increase in the marine environment appears to be limited only by prey availability.

Science, this issue p. 1367; see also p. 1316

View the article online

<https://www.science.org/doi/10.1126/science.aax9044>

Permissions

<https://www.science.org/help/reprints-and-permissions>

Use of this article is subject to the [Terms of service](#)

Science (ISSN 1095-9203) is published by the American Association for the Advancement of Science. 1200 New York Avenue NW, Washington, DC 20005. The title *Science* is a registered trademark of AAAS.

Copyright © 2019 The Authors, some rights reserved; exclusive licensee American Association for the Advancement of Science. No claim to original U.S. Government Works